SUBMITTED FOR REVIEW OMAE PAPER 28075

VIV response of long free spanning pipelines

by

Finn Gunnar Nielsen, Norsk Hydro

Tore H Søreide, Reinertsen Engineering

Stig Olav Kvarme, Reinertsen Engineering

Abstract.

Vortex induced vibration (VIV) of free spanning pipelines in current is considered. In standard VIV estimation, one mode of oscillation is considered only. Increasing the length of the span, several modal shapes may be excited. Further, due to the sag effect of a long free span, the dynamic properties in vertical and horizontal direction of the span are different. This causes a much more complex VIV response pattern for long free spans than for short spans. The observed VIV response of long free spans during model testing is discussed. Hypotheses that may explain the observed behaviour are presented. Also a format of new design principles for long free spans is outlined.

Nomenclature

A	Vibration amplitude
A_0	Initial sag amplitude
A_{2D}	2D added mass
B	Damping
C	Restoring
D	Pipe diameter
EI	Bending rigidity
F	Excitation force
f_{0CF}, f_{0IL}	Cross-flow and in-line eigenfrequencies
K_n	Secant stiffness for mode n.
m	Mass of pipe per unit length. Including content.
m, n	Mode numbers for in-line and cross-flow direction.
N_0	Initial effective pipe tension
u	Current velocity
U_r	Reduced velocity
U_s	Relative velocity at point of separation
t	time
$y(t), z(t)$	In-line and cross-flow vibration
y_a, z_a	Modal amplitudes
x	Axial coordinate along span.
w	Displacement along span
ω	Circular frequency of oscillation
ω_0	$= 2\pi f_0$ Circular natural frequency in calm water
L	Length of span
φ	Phase angle between in-line and cross-flow response
ϕ	Modal shape function

ρ	Density of water
ς	Relative damping
ΔA	Additional added mass at lock-in.
Γ	Vortex strength

Introduction.

Several new oil and gas fields in deep water are facing a very irregular seabed condition. One particular example is the Ormen Lange field offshore West Norway in the Norwegian Sea. Installation of a gas pipeline in this area results in a large number of free spans, some of which will have length to diameter ratio (L/D) beyond currently accepted values. The length and height of the spans depend upon the pipe dimensions as well as the laying tension, Figure 1. An example of free spans along one particular pipeline route considered is shown in Figure 2. In the figure maximum span height versus span length is plotted. In the water depth considered, beyond 300m, waves will not impose forces of any significance to the pipeline. However, the ocean current causes a separated flow around the free spanning pipeline. In the separation process vortices are shed. These vortices induce oscillatory forces on the free span that result in horizontal and vertical oscillations. The horizontal oscillations are denoted in-line (IL) oscillations, while the vertical oscillations are denoted cross-flow (CF) oscillations. A standard procedure of estimating the magnitude of the IL and CF oscillations is outlined by Det Norske Veritas (1998) (DNV Guideline No. 14 to be updated in RP105 which will be issued in 2002). The DNV guideline is based upon state of art knowledge of VIV. A large number of laboratory tests under 2D flow conditions as well as a limited number of tests with finite span models are used to develop the guideline. The response of a free span of finite length is obtained by using the cross-flow principle for the incident current, i.e. considering the normal component of the current only. Further, at each cross-section of the pipe, it is assumed that the flow is two-dimensional. By using a modal weighting of the response, the VIV response along the span is obtained. The details are outlined in e.g. Blevins (1977).

Current practise for free span design is relevant for L/D ratios up to approximately 120. For spans with length below this value, the beam effect of the stiffness is significant and the modal shape of the oscillation is one half wave over the length of the span. Also the eigenfrequencies in IL and CF directions are almost equal. For spans with L/D ratio much larger than this, say beyond 200, the cable effect contributes significantly to the stiffness, see e.g. Søreide, Paulsen and Nielsen (2001). This implies that the dynamic properties of the free span in IL and CF direction differ. As the length of the span increases, more eigenfrequencies may be in the range of VIV excitation. I.e. we have to decide which mode shapes are present and which mode shapes dominate the response.

In the following a summary of some experimental results for VIV response for long free spans is presented. Some of the observations and hypotheses on why the response of long free spans differ from what should be expected from 2D tests are evaluated. The effect of the sag of the free span on the eigenfrequencies and dynamic effects is also addressed.

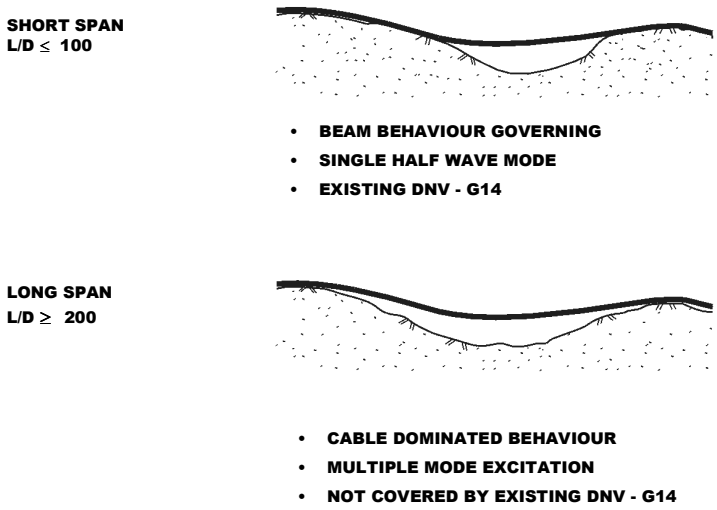

Figure .1 Examples of free spans. Top: Short span where the dynamic is governed by beam behaviour. Bottom: Long span where the cable effect is important.

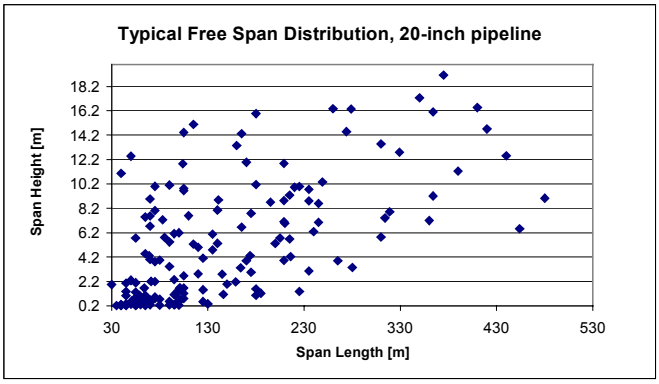

Figure 2. Distribution of length and height of free spans along one specific pipeline route on the Ormen Lange field. 20-inch pipeline installed by S-laying.

Model tests.

Model tests with long free spans were performed in the ocean laboratory at Marintek, Trondheim in December 2000. A second set of tests where made in December 2001. Figure 3 illustrates the test set-up. A truss girder of length 12m serves as the support structure for the pipe. At one end there is a mechanism for pretension and axial stiffness variation, while the other end is instrumented for axial force measurement. The model is restricted at the ends with respect to torsional rotation, thereby retaining curvature measurements in horizontal and vertical directions, respectively.

Four different spans were modelled. The lengths were L = 4.7m, 7.0m, 9.0m and 11.4m. By the model scale of 17.05, these spans in full-scale range from 80 m to 195 m, thereby representing L/D-ratios from 145 to 350. The shortest span is close to the length up to which DNV G14 presently is applicable. The mass ratio for the model was $m_p / \frac{\pi}{4}\rho D^2 = 1.40$.

The variation of the span is obtained in the model set up by adding supports along the two end parts of the 11.4 m span. The boundary condition simulated for the shorter free spans is thereby a partially clamped end condition, while for the 11.4m span, rotationally free end supports are simulated. All the results presented in the following are from tests where the rig is towed in calm water. The towing direction was perpendicular to the span. Further details about the test set-up are given by Søreide et al. (2001).

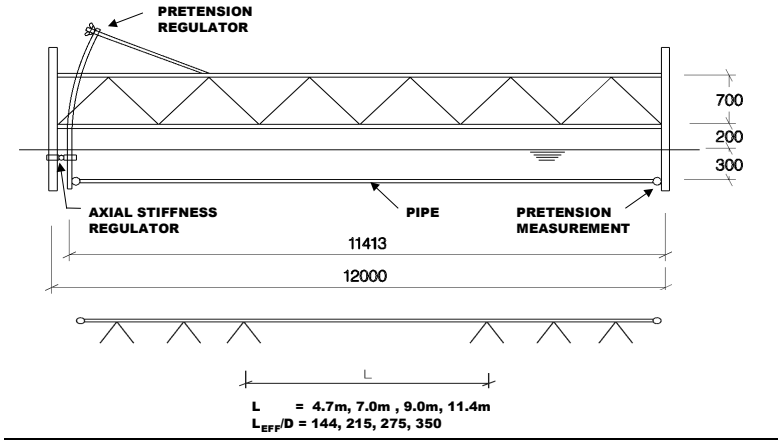

Figure 3. Model test arrangement with support structure and system for adjusting pretension and axial stiffness. Bottom: The supports used for modelling shorter spans.

Test Results.

In the following a few examples of the experimental results are presented. In Figure 4 the cross flow and inline responses (A/D) for a span with L/D = 145 are presented as function of the full-scale velocity. In this case the beam effect is the major stiffness contribution. The cross-flow as well as the in-line response are dominated by the first mode (one half-wave length). The CF response is close to what is observed in 2D tests. The maximum response is similar to the estimate given by DNV G14, but the slope of the response curve is lower. The presented amplitude is the equivalent 2D amplitude, i.e. the modal amplitude divided by the modal shape factor. In this case we have assumed a sinusoidal mode shape, resulting in a shape factor of 1.16.

DNV G14 handles basically the first mode in cross-flow and inline, respectively. In Figures 4 and 5 the format of DNV G14 is also applied to the higher modes, by introducing the actual eigenfrequencies in the reduced velocity.

The in-line response follows the DNV guideline in the "pure" in-line response range. When the cross-flow response increases, a cross-flow induced in-line response is observed. The magnitude of this response is in the order of 40% of the cross-flow response. In Figure 5 results for a long span (L/D = 350) are presented. The stiffness is in this case dominated by cable and sag effects, see the discussion on stiffness contributions below. Due to the sag effect in the span, the second mode (two half-wave lengths) has lower eigen-frequency than the first mode. The cross-flow response has a second mode response at low velocities. At higher velocities, the cross-flow oscillations switch to a first mode response. We observe that the maximum cross-flow modal amplitude is significantly less than predicted from DNV G14.

The in-line response can, according to DNV G14 take several modal shapes. In this specific case, the 3rd mode (three half-waves) dominates the in-line response for most velocities. In general the cross-flow induced in-line response is less than 50% of the cross-flow response.

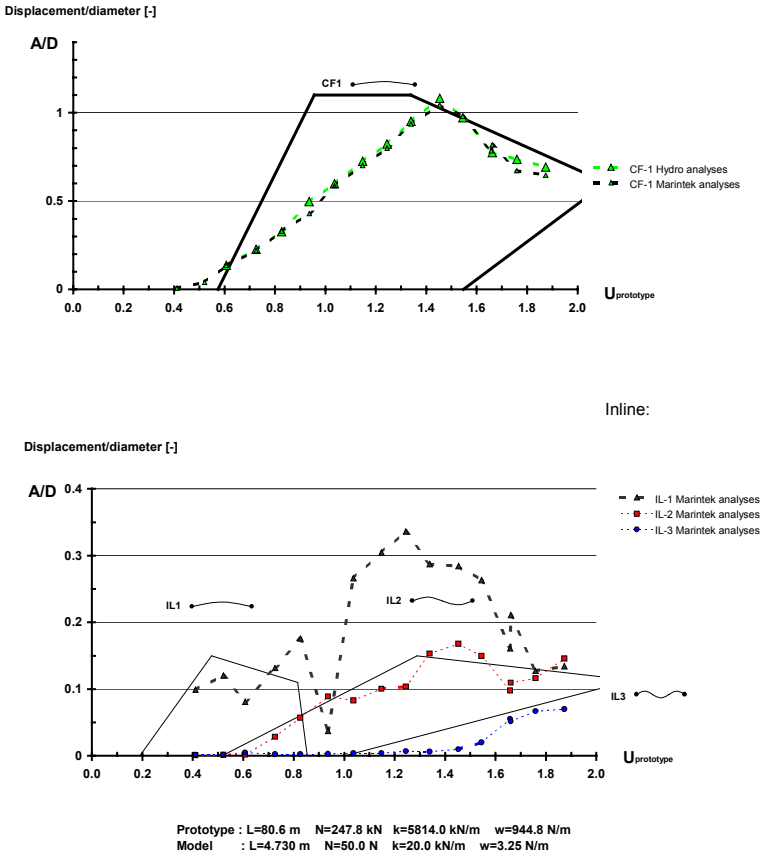

Figure 4. Cross-flow (top) and in-line (bottom) response for a span with L/D = 145. The solid lines denoted CF1 and IL1, IL2, IL3 are the response level expected using DNV G14. The dashed lines are measured responses. The modal contributions are computed using two different techniques.

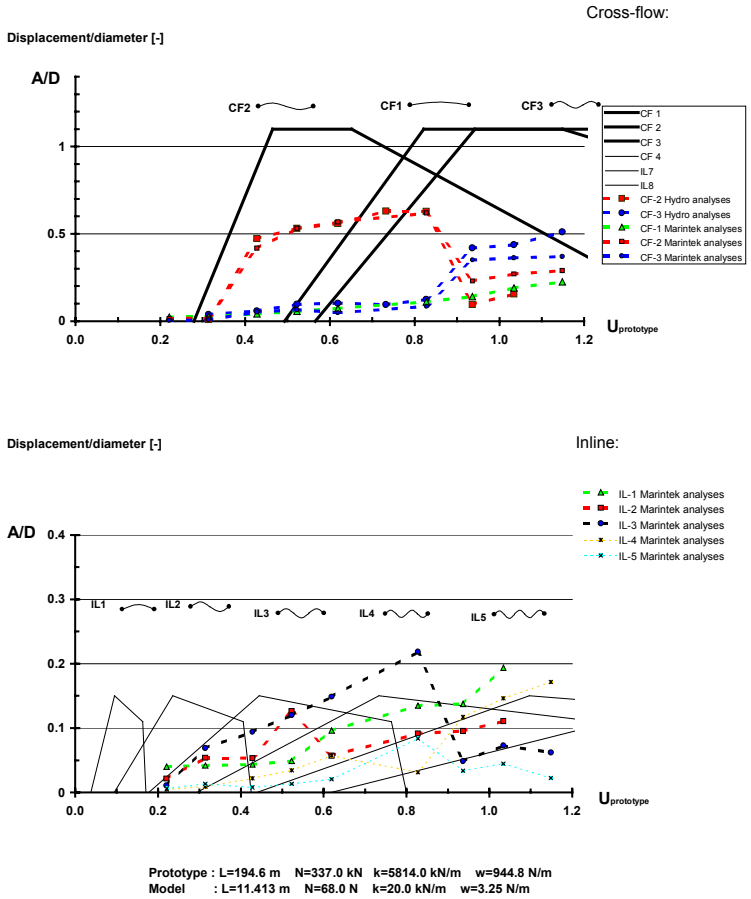

Figure 5. Cross-flow (top) and in-line (bottom) response for a span with L/D = 350. The solid lines denoted CF1, CF2 and CF3 (IL1, IL2 ..) are the response levels expected using DNV G14. The dashed lines are measured responses. The modal contributions are computed using two different techniques.

Observations from tests.

The response curves used in DNV G14 are based mainly on results from 2D tests. One observation that can be made from 2D tests as well as 3D tests with short (beam controlled) spans is that the cross-flow response depends upon the in-line response. If the IL response is restricted, a more rapid build-up of the CF response at low reduced velocities, U_r is observed. The DNV G14 as well as most empirical theories give a response build-up that is similar to the in-line locked condition.

The difference in response with and without the cylinder free to respond in the in-line direction must be related to the forces generated by the vortex shedding process from the cylinder. The time derivative of the shed vorticity, Γ on a 2D cylinder is given by:

$$\frac{d\Gamma}{dt} = \tfrac{1}{2} U_s^2 \qquad (1)$$

Here U_s is the fluid velocity at the point of separation. The shed vorticity excite forces on the cylinder. If we consider a linear single degree of freedom system excited by a harmonic force at resonance, the exciting force must balance the damping force and thus be 90 degree out of phase with the excursion. However for VIV, it is observed that the frequency of oscillation may differ from the calm water resonance frequency, see Figure 6. Similar observations are made by e.g. Larsen et al. (2001). The cross-flow dynamic equation may thus be written as:

$$(m + A_0 + \Delta A)\ddot{z} + B\dot{z} + Cz = F_{CF}(t) \tag{2}$$

As the system oscillates at resonance we have that the exciting force is balancing the damping: $B\dot{z} = F_{CF}(t)$. The inertia force related to the calm water added mass, $-A_0\ddot{z}$, is related to the ideal fluid (non-separated) flow. The vortex shedding process is thus responsible for the additional inertia force, $-\Delta A\ddot{z}$. Alternatively the system can be defined as non-resonant and $-\Delta A\ddot{z}$ added to the right hand side of the equation. According to Larsen et al. ΔA may take values in the range $[-1.6A_0, 1.2A_0]$. The ratio between the inertia and exciting force is given by:

$$\frac{\omega^2 \Delta A z}{\omega^2 (m + A_0)\omega_0 \varsigma z} = O\left(\frac{\Delta A}{4A_0\varsigma}\right) \tag{3}$$

In this order of magnitude estimate it is assumed that the frequency of oscillation is close to the calm water natural frequency and the pipe is close to neutral. From (3) we thus observe that for a lightly damped system, the inertia force due to the vortex shedding is large compared to the exciting force. I.e. the magnitude of the cross-flow force due to vortex shedding is considerably larger than necessary to balance damping. A minor phase shift of the total force may thus alter significantly the exciting part of the force, i.e. the force in phase with the velocity. The magnitude and phasing of the in-line vibrations may cause a phase shift in the vortex shedding pattern. It is to be expected that the cross-flow response will be affected by this change in forcing.

For short span lengths, the phasing between the in-line and cross-flow response is similar to that observed in 2D tests, see Figure 7. In this figure trajectories of in-line versus cross-flow excursions are plotted for similar reduced velocities, $U_r = \frac{u}{f_0 D}$. We observe that the in-line motion has twice the frequency of the cross-flow motion. Assume that the cross-flow and in-line motions for the 3D cases may be written as:

$$\begin{aligned} y &= y_a \cos(2\omega t + \varphi)\sin\left(\frac{m\pi x}{L}\right) \\ z &= z_a \cos(\omega t)\sin\left(\frac{n\pi x}{L}\right) \end{aligned} \tag{4}$$

Here *n* and *m* represent the number of half waves along the span in cross-flow and in-line direction, respectively. For the 2D cases the sine-functions are to be replaced by unity.

From Figure 7 we observe that the phase angle φ in (4) is in the range $0 - \frac{\pi}{4}$ both for the 2D and 3D tests. We also observe that some higher harmonic components of oscillation are present, however, these do not change the general picture of the oscillation pattern. In the actual 3D case both the in-line and the cross-flow oscillations are dominated by the first

mode, i.e. *m*=*n*=1. Plotting the y-z excursion at different cross-sections of the free span, similar patterns as in Figure 7 appear.

In Figure 8 trajectories of the in-line versus cross-flow excursions for a span with L/D = 350 are presented. The trajectories are presented for different cross-sections of the span and for two different reduced velocities. We observe that the trajectories vary between the different cross-sections. Analysing the tests we find that for $U_r = 3.6$ the cross-flow response is dominated by the second mode (n=2), but also has some contribution from the first mode. In in-line direction the third mode (m=3) dominates. The same modes are dominating the response for $U_r = 6.8$.

The slope of the cross-flow motion versus reduced velocity in the 3D modal responses is similar to what is observed in 2D tests with the in-line mode free. However, the maximum cross-flow response is significantly less than obtained in 2D tests. This is the case for all the 3D tests except the shortest span. In that case the response pattern corresponds to *m=n=1*. In most other cases we obtained $m < n$, n= 2 and m=3 is the most frequent combination. For the long spans more than one mode shape may be present simultaneously.

From (2) we may compute the total relative velocity between the fluid and cross sections of the span. Assume that the force due to vortex shedding is related to the time derivative of the shed vorticity (1). We then may obtain a modal force proportional to the square of the relative velocity between cylinder cross section and water. I.e. the modal force is assumed to be proportional to U_s^2 weighted by the modal shape in cross-flow oscillation. However, if this force is acting as an excitation force or as a contribution to added inertia, depends on the phasing between the vortex shedding process and the motion. From a hydrodynamic viewpoint it is likely that this phasing depends upon the magnitude as well as phase of the in-line motion relative to the cross-flow motion. In cases where the modal shape of the in-line motion differ from the modal shape of the cross-flow motion it is therefore to be expected that the modal excitation force will be reduced. By assuming characteristic in-line and cross-flow motion amplitudes at $U_r = 2\pi$, rough estimates based upon the above considerations indicate that the cross-flow excitation force with *m=2, n=1* is about 60% of the excitation force with *m=n=1*.

The tests came out with curvatures for inline and cross-flow directions, respectively, as function of current velocity for ten sections along the pipe. These results indicate a close to linear relationship between curvature and velocity, indicating also the same relation for strain and stress ranges along the pipe. As the strain energy within a vibration mode of the pipe goes as a quadratic function of stress amplitude, the discussion of an energy approach instead of the displacement based VIV format has been raised. However, further details remain before the analysis scheme is available. Considering stresses directly would simplify the procedure for fatigue calculation.

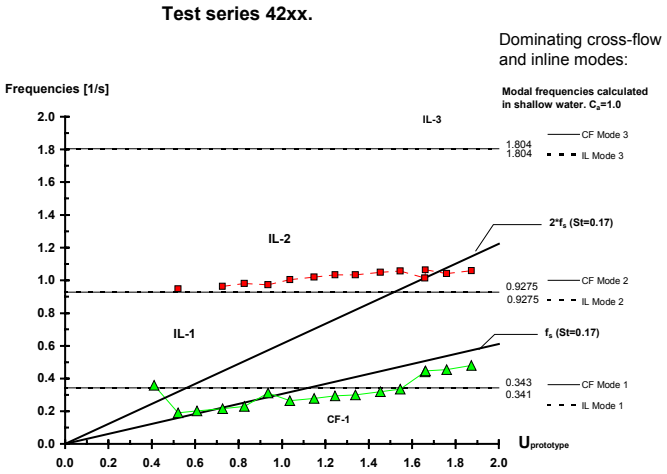

Figure 6. Cross-flow and in-line frequency of oscillation for a span with L/D =145, ref. Figure 4.

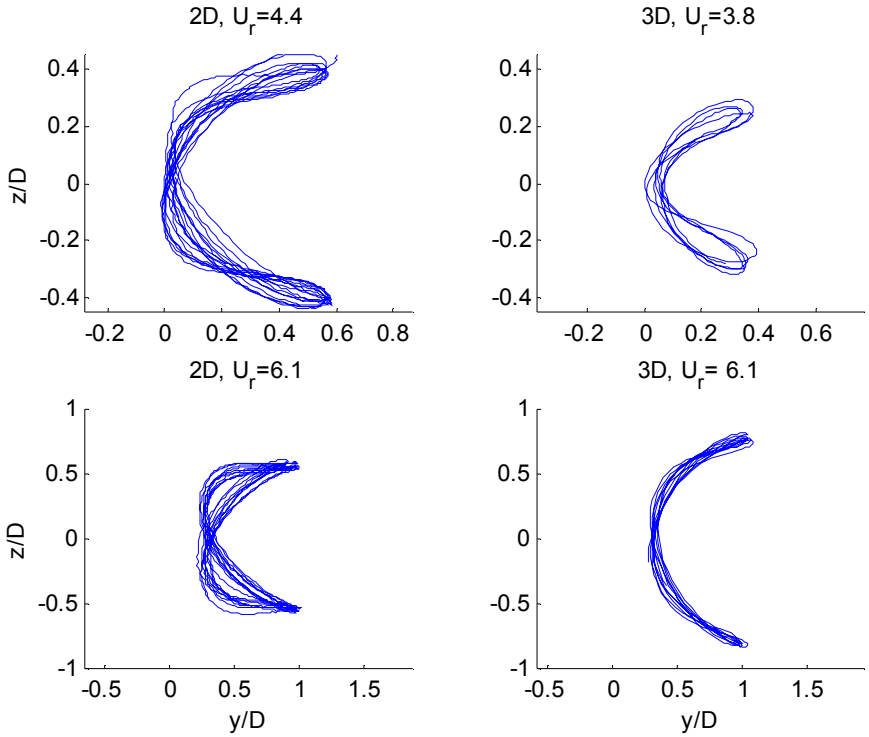

Figure 7. Trajectories of in-line versus cross-flow motion. Left figures: results from 2D tests. Right figures: Mid-span excursion for free span with L/D = 145.

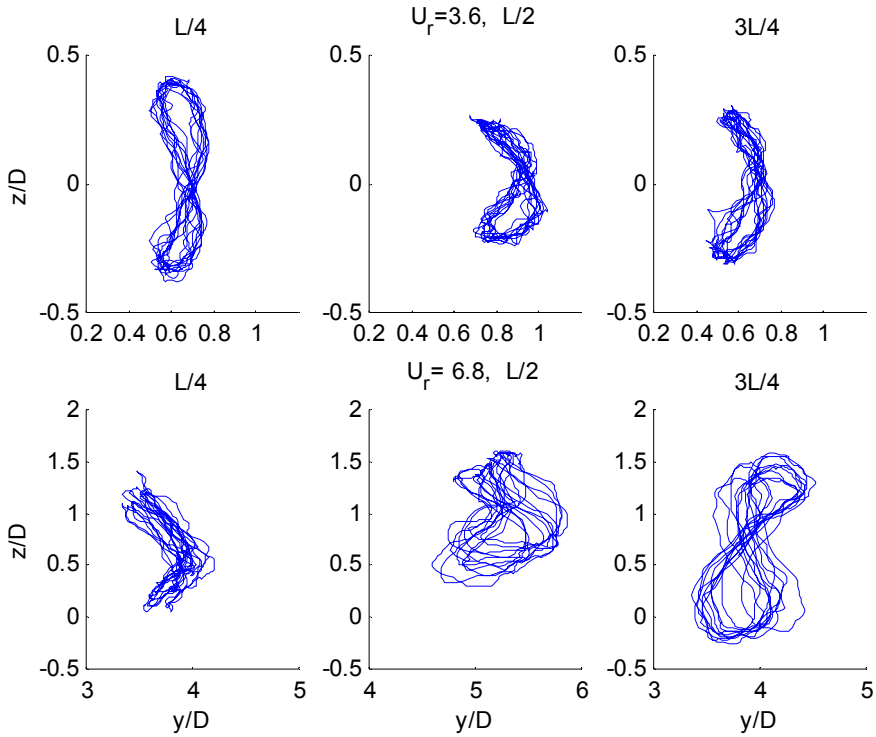

Figure 8. Trajectories of in-line versus cross-flow motion. Free span with L/D = 350. Motions at quarter span, mid-span and three-quarter span. Top: U_r=3.6. Bottom: U_r=6.8.

Hypotheses of Cross-flow / In-line interaction.

Based upon analyses of a large amount of model tests of long free spans, hypotheses and preliminary procedures for estimating the in-line and cross-flow response have been established. We classify the length of the spans by means of the lowest eigenfrequencies:
"Short" spans have beam dominated behaviour, i.e. the first CF and IL eigenfrequencies are approximately equal, $f_{01CF} \approx f_{01IL}$ Further, the second in-line eigenfrequency $f_{02IL} > \alpha f_{01CF}$. For a pure beam we have $f_{02IL} = 4 f_{01CF}$. To have "beam-like" behaviour it is assumed that $\alpha \gtrsim 3.5$ is sufficient.

For "Intermediate spans", the cable effects become important, i.e. $\alpha \lesssim 3.5$. Still however, the first CF mode (One half-wave length) and either the first or second (two half-wave length) IL mode dominate the VIV response of the span. The results presented in Figure 4 are for a span of intermediate length.

For "long spans" the CF mode of lowest frequency can be either the first or the second mode. Further, using DNV G14, more than one CF mode can exist in the actual current velocity range. The results presented in Figure 5 are for a long span. Further discussions on the eigenfrequencies are given below.

The hypotheses for estimating the CF and IL modal responses are based upon the following:

In general the CF and IL modal responses are estimated by use of the DNV G14. However, a reduced slope of the CF response is proposed. Further the response curves are corrected to account for the actual Strouhal number. The cross-flow induced IL response is estimated to approximately 40% of the CF response.

In the start-up region, U_r in the range 2 - 4, the velocity of the IL response is larger than the velocity of the CF response. We denote this range the IL-controlled range. The IL eigenfrequency controls the oscillations and the CF oscillations are non-resonant at half the IL response frequency.

As the CF response amplitude increases, the CF velocity takes control over the vortex shedding process. The CF frequency of oscillation is estimated by a similar procedure as outlined in Larsen et al. (2001) However, a larger peak value in added mass is included to account for the high added mass values at low CF response amplitudes. In the CF controlled range the IL response is non-resonant at twice the CF response amplitude.

The mode shape of the IL response is found by assuming that the mode shape with corresponding eigenfrequency closest to the actual frequency of IL oscillation is preferred. If the IL mode shape is different from the CF mode shape, the maximum CF response amplitude is limited to approximately *0.7D*.

Having considered all modal candidates to the CF response, the one with largest estimated amplitude is assumed to take control of the process. The remaining modes are suppressed.

This procedure has several common ideas to state of art VIV estimating tools. The main difference is related to inclusion of the IL response in the considerations. In Figure 9 is given an example of the estimated and measured responses for intermediate span. The estimates reproduce the main features of the measured modal response, even if the IL response in general is overestimated.

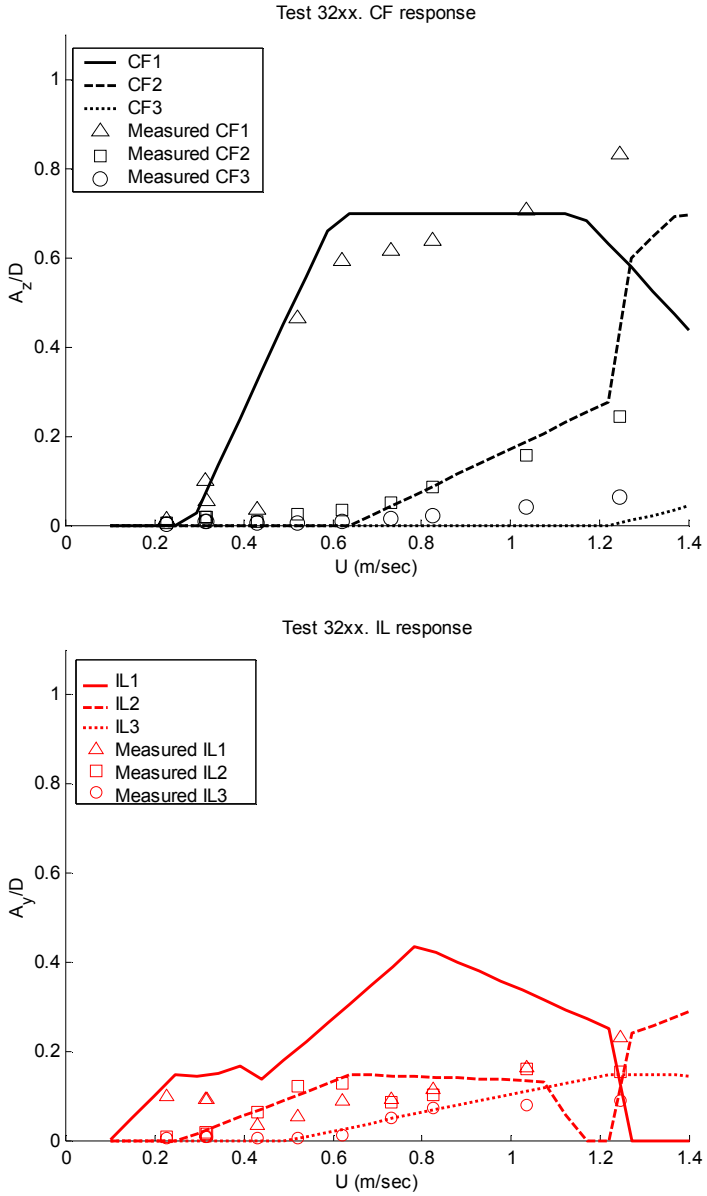

Figure 9. Measured and estimated CF (top) and IL (bottom) responses for a span with L/D = 220.

Effect of non-linear restoring forces

We want to evaluate if non-linear restoring effects related to sag and axial force variations may have importance to the observed dynamics. Consider a free span with sag as illustrated in Figure 10. For simplicity assume a sinusoidal initial displacement in vertical direction:

$$w_0(x) = A_0\phi(x) = A_0 \sin\left(\frac{\pi x}{L}\right) \tag{5}$$

The dynamic displacement adds to the static displacement. Again a sinusoidal mode shape is assumed:

$$w_n(x) = A\phi(x) = A\sin\left(\frac{n\pi x}{L}\right) \quad n = 1,2,... \tag{6}$$

Here A is the dynamic amplitude of oscillation and n the number of half-waves along the span. The secant stiffness for the modal displacement, K_n can be shown to be:

$$\begin{aligned} K_1 &= \frac{\pi^4}{2L^3}EI + N_0\frac{\pi^2}{2L} + k\frac{\pi^4}{8L^2}\left[A_0^2 + \tfrac{3}{2}A_0A_1 + \tfrac{1}{2}A_1^2\right] \quad \text{for } n = 1 \\ K_n &= \frac{n^4\pi^4}{2L^3}EI + N_0\frac{n^2\pi^2}{2L} + k\frac{n^4\pi^4}{16L^2}A_n^2 \quad \text{for } n > 1 \end{aligned} \tag{7}$$

These expressions are valid to second order in A. EI is the bending stiffness of the pipe, N_0 is the mean effective tension in the pipe and k is the axial stiffness at each of the shoulders, including axial stiffness of one half of the pipe span. The first term on the right hand side of (7) is due to the bending stiffness of the pipe. This term decays rapidly with the length of the span. The second term is due to the effective axial tension, i.e. the normal straight cable effect. The third term is due to the combined effect of axial stiffness and mean sag. For the first CF mode (one half-wave) displacement there are interaction terms between the initial and dynamic displacement. These terms give linear as well as non-linear contributions to the dynamic restoring force. The first term in the brackets on the first line of (7) gives a linear restoring force that increases rapidly with the initial displacement. The last two terms give a quadratic and cubic restoring force respectively.

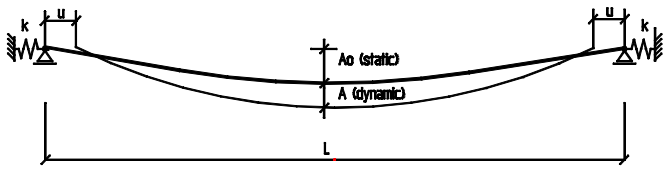

Figure 10. Model used in considering non-linear restoring effects

If we consider the in-line displacement, with $A_0 = 0$, or modes with more than one half wavelength along the span, all terms involving the initial displacement vanishes. Only the non-linearity corresponding to the dynamic amplitude remains. This is the last term in (7). The stiffness due to the beam effect as well as the non-linear shoulder effect increases rapidly as the mode number increases.

If $A_0 >> A$, the linear sag-axial stiffness contribution is much larger than the two non-linear terms. I.e. the non-linearities are not expected to give significant contributions to the modal restoring force in a span with large sag.

The modal mass, M is for all modes obtained as:

$$M = \frac{mL}{2} \tag{8}$$

Here *m* is the mass per unit length of the pipe. In our application we have included the added mass with $C_m = 1$.

The un-damped eigenfrequency in submerged condition, for mode n, ω_n is obtained as:

$$\begin{aligned} \omega_1 &= \sqrt{\frac{K_{lin}}{M}} = \frac{\pi}{L}\sqrt{\frac{N_0}{m}\left(\frac{\pi^2 EI}{L^2 N_0} + 1 + \frac{\pi^2}{4L}\cdot\frac{kA_0^2}{N_0}\right)} \quad \text{for } n = 1 \\ \omega_n &= \frac{n\pi}{L}\sqrt{\frac{N_0}{m}\left(\frac{n^2\pi^2 EI}{L^2 N_0} + 1\right)} \qquad\qquad \text{for } n > 1 \end{aligned} \tag{9}$$

Here K_{lin} is the linear part of *K*.

In the above expressions a sinusoidal mode shape has been assumed for the initial as well as the dynamic excursion. This provides a good approximation for moderate shoulder stiffness. However, for very large shoulder stiffness, the dynamic deformation mode will differ from the sinusoidal shape and consequently (9) will over-predict the natural frequency for n=1. See Søreide et al. (2001). Hover and Triantafyllou (1999) give a complete solution to the natural frequencies of a curved tensioned elastic beam.

To investigate the influence of the non-linear stiffness terms on the VIV amplitude of oscillation, the following experiment is made: We assume the span behaves as a single degree of freedom oscillator. A linear damping *B* is assumed. Neglecting the non-linear restoring terms, we find a modal excitation force corresponding to a response amplitude of one diameter (D). This is characteristic maximum response amplitude in cross-flow vibration. The amplitude of the modal excitation force is given as:

$$F_A = \omega_0 AB \tag{10}$$

Next, we excite the non-linear system with the same harmonic force, $F = F_A \cos(\omega_0 t)$. The response is computed by a time domain simulation. Thereby the effect of non-linear restoring may be estimated. We consider a long free span case as given in Table 1. To obtain a dynamic response of A/D=1, a harmonic oscillation amplitude of 1.4367E04 N is applied. The results are summarised in Table 2: The computed response amplitude including non-linear restoring is within 3% of the linear case. The non-linear restoring forces contribute less than 7% to the total restoring force. It is thus concluded that the non-linear restoring effects do not have any practical significance to the VIV dynamics in this case. The conclusion is similar for other relevant combinations of parameters.

Table 1. Particulars of the span considered.

Mass of pipe per unit length, m = 602 kg/m
Length of span, L= 194.6 m
Bending stiffness, EI = 2.99E08 Nm^2
Initial sag, A_0 = 11.51 m.
Axial stiffness of shoulders, k = 5.814E06 N/m
Effective tension in pipe, N_0 = 3.45E05 N
Linear Damping, $B/(\omega_0 mL) = 0.05$
Diameter of pipe, D = 0.556 m

Table 2. Simulated maximum and minimum response, A/D and maximum contribution to restoring force.

	Max(A/D)	Min(A/D)	Max restoring contribution (N)
Linear restoring	**1.006**	**-1.008**	**143.7E03**
Quadratic restoring	**0.982**	**-1.031**	**10.0E03**
Cubic restoring	**0.982**	**-1.031**	**0.16E03**

Conclusions

Model tests on long free spans have revealed that the VIV response of short spans with beam like behaviour is similar to what is observed in 2D VIV tests. For longer spans, the interaction between in-line and cross-flow VIV responses becomes important. The modal shape of the in-line response may differ from the cross-flow response. This will reduce the correlation of vortex shedding along the span, causing reduced cross-flow response.

A procedure for including the above effects in design is outlined. The procedure is based upon present guidelines for estimating VIV response of free spanning pipelines. The procedure captures the main features of the measured modal response.

Non-linear restoring effects due to shoulder stiffness and sag are discussed. The non-linearities are found not to be important to the VIV response for the cases considered.

Acknowledgements

The Ormen Lange partners, BP, Exxon, Norsk Hydro, Petoro, Shell and Statoil are all acknowledged for allowing us to publish these results. We also acknowledge the members in the specialist group for long free span design in the Ormen Lange license for valuable contributions in the discussions on the interpretation of the model test results.

References

Blevins, R.D., 1977: Flow-induced Vibrations. Van Nostrand Reinhold Company.

Det Norske Veritas, 1998: Free spanning Pipelines, Guideline No. 14. Det Norske Veritas, Høvik, Norway.

Hover, F.S. and Triantafyllou, M.S., 1999: Linear Dynamics of Curved Tensioned Beams. Journal of Sound and Vibration. 228, 923 -930.

Larsen, C.M., Vikestad, K., Yttervik, R. and Passano, E., 2001: Empirical model for analysis of vortex induced vibrations - Theroretical background and case studies. Proceedings of 20th International Conference on Offshore Mechanics and Arctic Engineering, OMAE 2001, Rio de Janeiro, Brazil.

Søreide, T. H., Paulsen, G. and Nielsen, F.G., 2001: Parameter Study of Long Free Spans. ISOPE 2001, Stavanger, Norway.